DTI reveals abnormal white matter pathways to classic language areas in semantic dementia

J. Acosta-Cabronero[1], K. Patterson[1], T. D. Fryer[1], J. R. Hodges[2], G. Pengas[1], G. B. Williams[1], and P. J. Nestor[1]
[1]Department of Clinical Neurosciences, University of Cambridge, Cambridge, Cambridgeshire, United Kingdom, [2]Neuroscience Research Australia, Randwick, Australia

Introduction: Semantic dementia (SD), in which there is progressive deterioration of semantic knowledge, is associated with focal, typically asymmetric, temporal lobe degeneration (Desgranges et al., Neurobiol Aging 2007; Hodges et al., Brain 2010). The ventro-rostral temporal lobe is most severely affected and there is concordance between atrophy and reduced metabolic activity (Chan et al., Ann Neurol 2001; Davies et al., Eur J Neurosci 2004; Nestor et al., Neuroimage 2006). We confirmed the veracity of this claim using [^{18}F]-fluorodeoxyglucose positron emission tomography and anatomical magnetic resonance images. However, the novel aspect of the current study was to shed new light on the neuronal projections from the ventro-rostral temporal cortex lesion by studying the full extent of white matter (WM) changes using diffusion tensor imaging (DTI) with no *a priori* assumptions about the nature or spatial location of the tracts involved. **Methods**: Ten patients with a clinical diagnosis of SD according to consensus criteria (Neary et al., Neurology 1998) were recruited from the Memory Clinic at Addenbrooke's Hospital, Cambridge. Cognitive assessment of the patients revealed the usual SD pattern of largely preserved non-semantic abilities (such as digit span, visuo-spatial processing, etc), paired with significantly reduced performance on any test requiring semantic knowledge e.g. picture naming=25.5/64 (stdev=16.7), word-picture matching=46.1/64 (14.2), and picture-picture associative matching=41.3/64 (8.6). Twenty-one age- and sex-matched controls were also recruited. Diffusion datasets were acquired on a Siemens Trio 3T system with a 12-channel phased-array TIM head-coil using a twice-refocused, single-shot, echo-planar imaging pulse sequence (Reese et al., MRM 2003): TR/TE/NEX=7800 ms/90 ms/1; matrix, 96×96; 63 contiguous axial slices; isotropic voxel resolution of 2×2×2 mm^3; bandwidth of 1628 Hz/pixel and echo spacing of 0.72 ms. The tensor was computed using 63 non-collinear diffusion directions (b=1000 s/mm^2), and one scan without diffusion weighting (b=0 s/mm^2). We allowed for parallel acquisition of independently-reconstructed images using GRAPPA (Griswold et al., MRM 2002) with an acceleration factor of 2 and 39 reference lines. The FMRIB software library (FSL v4.1) (Smith et al., Neuroimage 2004) was used to correct for eddy currents; fit the diffusion tensor; and compute diagonal elements (L_1 or axial diffusivity, L_2 and L_3), mean diffusivity (MD) and fractional anisotropy (FA) at each brain voxel. $(L_2+L_3)/2$, known as radial diffusivity (RD), were also calculated. The tract-based spatial statistics (TBSS v1.2) approach (Smith et al., Neuroimage 2006), whereby the nearest most relevant tracts in each subject's spatially-normalised FA image are projected onto a skeleton, was used to perform voxelwise statistics at the tract centres only, hence minimising the effect of misregistration—a common problem that is compounded by atrophy. TBSS uses permutation-based non-parametric inference on unsmoothed statistical maps; 10,000 permutations of the data were generated to test against using 'randomise v2.1', and cluster-like structures were enhanced using the threshold-free cluster enhancement algorithm (Smith and Nichols, Neuroimage 2009). The statistical maps were corrected for multiple comparisons, with the threshold level set to family-wise error (FWE) corrected P<0.05; an uncorrected threshold of P<0.01 was also used for qualitative assessment. The abnormal (FWE-corrected) skeletonised voxels inferred from the most sensitive DTI metric were used to 'seed' the tractography algorithm. The most extensive TBSS result was deprojected onto each control subject's native DTI space to generate subject-specific 'seed masks'. The probabilistic diffusion tractography algorithm ('probtrackx') implemented in the FMRIB's diffusion toolbox (FDT v2.0) allows the computation of 'connectivity' distribution maps by incorporating a solution to the multiple fibre orientation problem ('bedpostx') (Behrens et al., Neuroimage 2007). In this study, 5,000 distance-corrected probabilistic pathways were computed using modified Euler integration for each 'seed voxel'. FA<0.2 and curvature (cosine of the minimum allowable angle: 0.2, or approximately 80°) stopping criteria were imposed; pathways were also terminated after 2,000 steps, using a step length of 0.5 mm. Tractographies computed for each control subject were projected back onto the spatially-normalised skeleton using the projection vectors inferred from the original FA data, and were then averaged. The resulting skeletonised 'connectivity' distribution map was finally thresholded to confine it to probabilities higher than 1% of the maximum possible number of probabilistic pathways in a voxel i.e. 5,000 × total number of 'seed voxels'. **Results and Discussion**: In a previous study, we reported TBSS results for decreased FA and increased absolute diffusivities in SD patients that confirmed that WM damage in SD is predominantly associated with inferior anterior temporal lobe neurodegeneration (Acosta-Cabronero et al., Proc ISMRM 2010). Anisotropy and absolute diffusion abnormalities showed overall concordance with each other, but differences in radial diffusivity were the most widespread. As expected, diffusion tensor abnormalities were also concordant with the structural and metabolic data (data not shown); hence aside from reinforcing the focal nature of ventro-rostral temporal lobe degeneration in SD, this tight coupling of diffusional WM changes with two markers of grey matter degeneration offers strong evidence that DTI in degenerative disease is a marker of axonal loss, which is largely assumed, but is lacking in evidence—DTI abnormalities could be driven by, for instance, glial changes. The average-control, skeletonised tractography 'seeded' with abnormal radial diffusivity voxels in SD (Figure, left column) featured pathways to remote areas such as (i) the orbito-frontal region through the uncinate fasciculus (UF); (ii) to the frontal lobe, via the superior temporal gyrus (STG), through the arcuate fasciculus (AF); and (iii) to the occipital lobe through the inferior longitudinal fasciculus (ILF). TBSS results for increased RD in SD patients at an uncorrected threshold level (P<0.01) revealed abnormalities extending further rostrally and dorsally through the UF and AF remote from the most severe alterations, but not further caudally through the ILF (Figure, right column). All other DTI metrics revealed the same remote alterations (at an uncorrected threshold level) along the UF and AF. In summary, there was contiguous involvement of WM pathways leading from the severely degenerated ventro-rostral temporal lobe to the supramarginal gyrus and the posterior STG—in other words, to the 'classic' posterior language areas, which are themselves spared (as demonstrated by the structural and metabolic results). We interpret these changes as representing degeneration of axons whose cell bodies arise in the former and project to the latter.

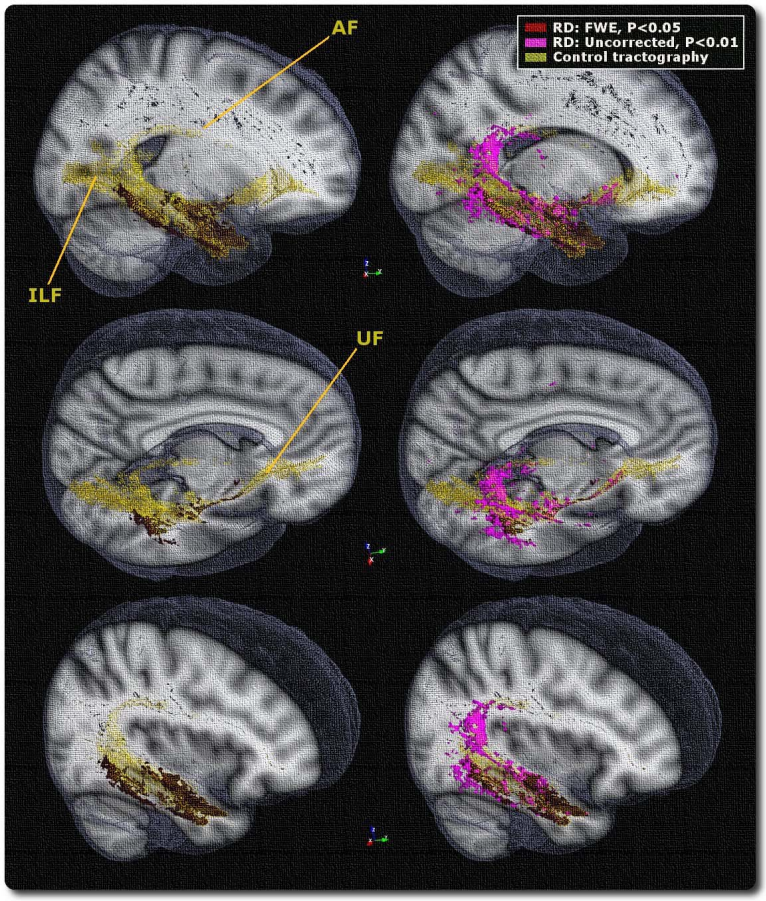

Conclusion: These findings offer direct evidence of how the ventro-rostral temporal lesion in SD—most notably the anterior fusiform (Binney et al., Cereb Cortex 2010; Mion et al., Brain 2010)—, proposed to be responsible for deteriorating semantic knowledge in semantic dementia and separate from 'classic' language areas, results in a loss of input to such language areas that are not directly lesioned.